

1 **Geometry and topology of Polish Outer Carpathian digital**
2 **elevation model interpreted lineament network in context of**
3 **regional tectonics**

4 Maciej Kania¹, Mateusz Szczęch¹

5 ¹Jagiellonian University in Kraków, Faculty of Geography and Geology, Institute of Geological Sciences,
6 Gronostajowa 3a, 30-387 Kraków, Poland

7 *Correspondence to:* Maciej Kania (maciej.kania@uj.edu.pl)

8

9 **Abstract.** The Polish part of the Western Outer Carpathians lineament network was analysed based on the
10 GMTED2010 digital elevation model. Lineaments were identified in the visual screening of the hillshade model.
11 To the best of our knowledge, no one has studied the geometrical properties of the network with relation to the
12 topological ones. The NetworkGT QGIS toolbox was applied to identify the nodes and branches of the network,
13 as well as to calculate the topology parameters. Our aim was to find differences between the western and eastern
14 parts of the Western Outer Carpathians; therefore, the analyses were carried out in six sectors chosen based on
15 the geographical subdivision in the geological context: three in the north, mainly the Silesian unit; and three in
16 the south, mainly the Magura unit. We found general agreement of the identified network with the
17 photolineament map; however, some of the photolineaments are not confirmed by digital elevation model
18 (DEM). We found that the topological parameters of the networks change from west to east, but not from north
19 to south. There are areas of increased interconnectivity, especially the Nowy Sącz Basin, where the lineament
20 network may reflect a complicated system of cross-cutting deep-rooted fault zones in the basement.

21 **1. Introduction**

22 Remote sensing imagery is an important source of data in regional tectonics, and its importance has been
23 growing in recent years. Since the 1970s, there have been multispectral satellite photos of the Earth surface
24 applied mainly in mineral mapping (e.g. van der Meer et al., 2012), as well as in tectonic studies (e.g. Leech et
25 al., 2003). The Shuttle Radar Topography Mission (SRTM) resulted in the first remote sensing digital elevation
26 model of most of the continental surface of the planet, with immense potential for application in geology (Yang
27 et al., 2011). Then, new superior resolution and quality models were created on both the global (satellite) and
28 local scale (mainly airborne LiDAR scanning). Digital elevation models are especially useful in areas with lush
29 vegetation. The application of LiDAR in the Carpathians' flysch-type mountains in geological interpretations
30 was shown, for example, in Kania and Szczęch (2022).

31 Our previous study (Kania and Szczęch, 2020), based on the interpretation of the model augmented with field
32 geological mapping (Szczęch and Cieszkowski, 2021), showed how a lineament network can be interpreted in
33 topological and geometrical terms. This paper presents to up-scale DEM-based geometrical and topological
34 analyses of a regional scale lineament network to find how this is reflected in the tectonic structure of the
35 Western Carpathians. Previous studies of the Carpathian lineaments were mainly focused on lineament strikes
36 distribution (e.g. Doktor and Graniczny, 1982, 1983; Doktor et al., 1985, 1990, 2002; Bażyński et al., 1986;
37 Graniczny and Mizerski, 2003); therefore, we decided to add an interconnectivity aspect in terms of the
38 topological parameters (Valentini et al., 2007; Sanderson and Nixon, 2015; Thiele et al., 2016), as a way of
39 better understanding the structural problems. There were two problems which we tried to address. The first aim
40 was to find, if and how the deep-rooted lineaments (fault zones) are influencing lineament network pattern on the
41 surface. Our hypothesis was that these deep-rooted features are expressed in the network independently of the
42 contemporary observed Carpathian nappes stacked structure. The second question was if and how the lineament
43 network properties change in the west – east profile. Most of the Carpathian-related studies are geographically
44 organised in mountain arc parallel belts, reflecting the main tectonostratigraphic units, now forming nappes and
45 being sedimentary basins during the Carpathian flysch depositions. We decided to keep this subdivision,
46 although combining this with physiographical subdivisions into sectors with borders perpendicular to the
47 Carpathian belt.

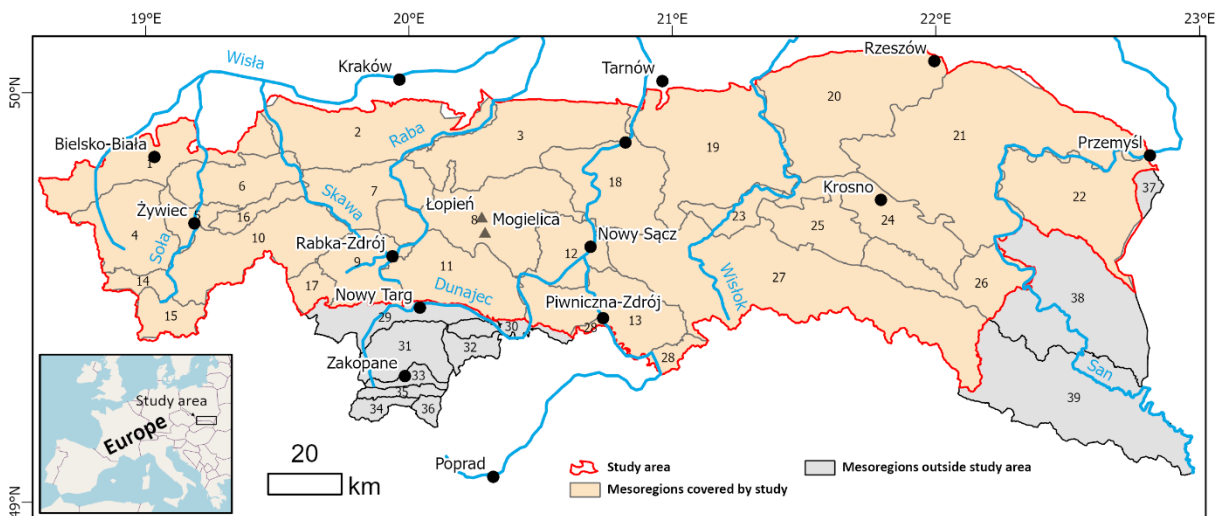
48 **2. Previous research on the Polish Outer Carpathian lineaments**

49 The fact that dislocation lines perpendicular to the Carpathian arc are related to the deep basement, and are
50 significantly older than the Carpathians themselves, was postulated even before the remote sensing era
51 (Teisseyre, 1907). The first modern attempts to interpret lineaments in the Polish Carpathians were based on the
52 Landsat MSS imagery and Heat Capacity Mapping Mission satellite, and reported together with data from the
53 whole territory of Poland on a photogeological map at 1:1 000 000 scale (; Bażyński et al., 1986; Graniczny and
54 Mizerski, 2003). The main lineament systems of the Western Carpathians in the context of structural geology
55 were shown by Doktor and Graniczny (1983) and Doktor et al. (1985). The results of satellite imagery lineament
56 detections were then correlated with geophysical data proving relationships between the surface, neotectonic
57 processes and deep Carpathian basement structure (Motyl-Rakowska and Ślącza, 1984; Doktor et al., 1990).
58 Airborne radar data were applied in tectonic analysis of the Carpathians, resulting in 17 000 short lineaments that
59 were the basis of the lineament density map (Doktor et al., 2002). The interpretation of SRTM hillshading
60 visualisation was performed by Chodyń (2004) on the limited area in Beskid Wyspowy Mts. Comparison of
61 Landsat MSS and SRTM data by Ozimkowski (2008) showed that whilst the main faults can be related to
62 lineaments, there are still numerous lineaments without geological explanation. In the last few years LiDAR high
63 resolution digital elevation models became available for the Polish Carpathians allowing more regional-scale
64 lineament network analysis and their interpretation as fault-related features (Kania and Szczęch, 2020, 2022;
65 Szczęch and Cieszkowski, 2021; Barmuta et al., 2021; Sikora, 2022)

66 **3. Study area**

67 The choice of the study area was based on the physiogeographical subdivision of Poland by Solon et al. (2018).
68 The following macroregions were selected: the Western Beskidy Foothills, Western Beskidy Mts., Orawa–
69 Podhale Basin, Mid-Beskidy Foothills and Mid-Beskidy Mts (Fig. 1). These five regions, with a total area of
70 17 437 km², cover most of the Polish part of the Outer Carpathians, excluding a small part of the Eastern Outer
71 Carpathians located in Poland.

72



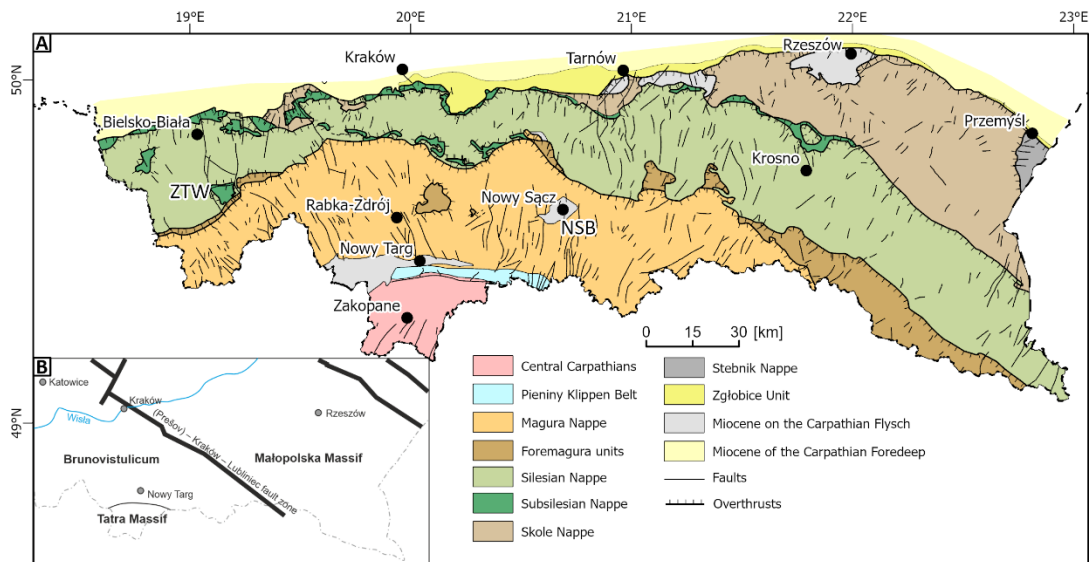
74 **Fig. 1. Physiogeographical subdivision of the study area and adjacent parts of the Polish Carpathians**
75 **based on Solon et al. (2018). Mesoregions covered by study: 1 – Silesia Foothills, 2 – Wieliczka Foothills, 3**
76 **– Wiśnicz Foothills, 4 – Silesian Beskid Mts, 5 – Żywiec Basin, 6 – Mały Beskid Mts, 7 – Makowski Beskid,**

77 **8 – Wyspowy Beskid, 9 – Orawa-Jordanów Foothills, 10 – Żywiec-Orawa Beskid Mts, 11 – Gorce Mts, 12**
78 **– Sącz Basin, 13 – Sącz Beskid Mts, 14 – Koniaków Intermontane Region, 15 – Żywiec-Kysuce Beskid**
79 **Mts, 16 – Pewel-Krzeczów Ranges, 17 – Orawa Interfluve, 18 – Rożnów Foothills, 19 – Ciężkowice**
80 **Foothills, 20 – Strzyżów Foothills, 21 – Dynów Foothills, 22 – Przemyśl Foothills, 23 – Gorlice Basin, 24 –**
81 **Jasło-Krosno Basin, 25 – Jasło Foothills, 26 – Bukowiec Foothills, 27 – Low Beskid Mts, 28 – Poprad**
82 **Foothills; mesoregions outside the study area: 29 – Orawa-Nowy Targ Basin, 30 – Pieniny Mts, 31 – Fore-**
83 **Tatra Foothills, 32 – Magura Spiska Mts, 33 – Sub-Tatra Depression, 34 – Western Tatra Mts, 35 –**
84 **Reglowe Tatra Mts, 36 – High Tatra Mts, 37 – Hermanowice Submontane Region, 38 – Sanocko-**
85 **Turczańskie Mts, 39 – Bieszczady Mts.**

86

87 **3.1 Geological setting of the study area**

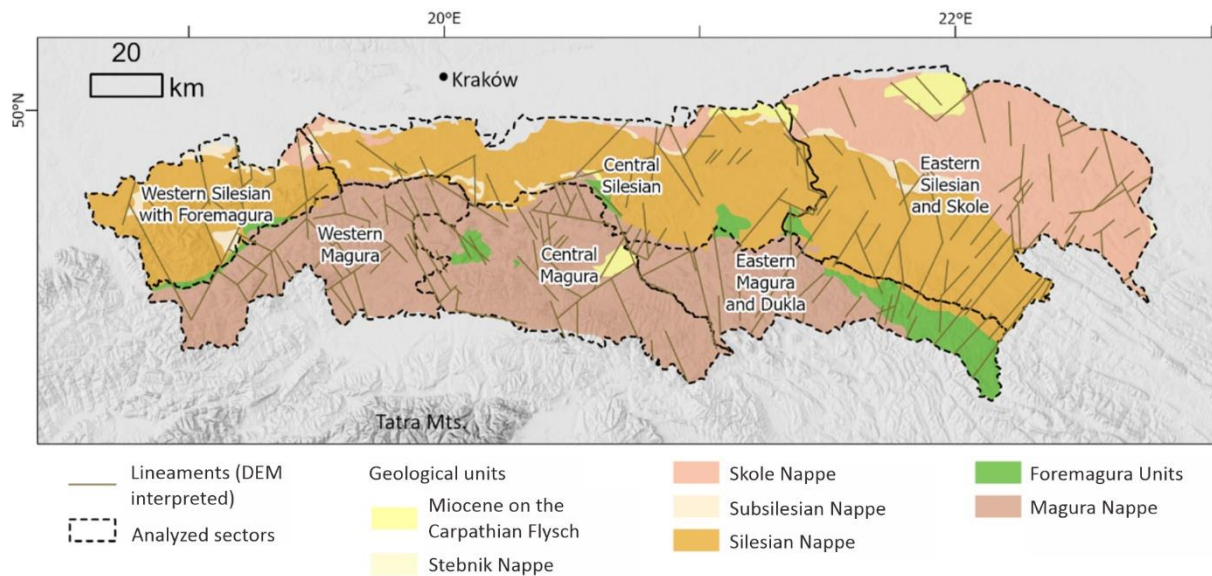
88 The research area is located in the Polish sector of the Western Outer Carpathians (Mahel', 1974; Książkiewicz,
89 1977; Ślącza et al., 2006; Fig. 2). It contacts tectonically with the Pieniny Klippen Belt from the south, which is
90 a border between the Outer and the Central Carpathians (Książkiewicz, 1977; Plašienka, 2018; Golonka et al.,
91 2019, 2021). The basement under the Western Outer Carpathians is formed of two blocks: Brunovistulicum and
92 Małopolska Massif, which are separated by major tectonic zone: Kraków – Lubliniec Fault (Fig. 2B) (Żaba, 1999;
93 Żelaźniewicz, 2011), cut by numerous other deep rooted lineaments (Doktór, 1985). The Outer Carpathians are
94 built mainly of flysch deposits, whose thickness is approximately 6 000 m, and thus they are also referred to as
95 the Flysch Carpathians (Książkiewicz, 1977; Golonka et al., 2005, 2021; Ślącza et al., 2006). These deposits are
96 Late Jurassic–Early Miocene in age and are mainly deep-sea sediments deposited by the gravity flow in the
97 several sedimentary basins of the Northern Tethys, separated by ridges (Książkiewicz, 1977; Golonka et al.,
98 2005, 2021; Ślącza et al., 2006). The thrust of the Central Carpathians block to the north on the European
99 Platform blocks — the Brunovistulicum and Małopolska Massif (Żaba, 1999) — led to the forming of the
100 synorogenic stage accretionary prism. The sediments deposited in the basins were folded and thrust one upon
101 another, creating the sequence of the nappes in the Miocene. Going from the south there are the Magura Nappe,
102 Dukla Nappe, Fore–Magura group of nappes, Silesian Nappe, Sub-Silesian Nappe and Skole Nappe (Mahel',
103 1974; Książkiewicz, 1977; Golonka et al., 2005, 2019; Ślącza et al., 2006). The deposits of the Outer
104 Carpathians are overthrust on the Miocene molasses filling the Carpathian Foredeep, which was deposited on the
105 front of the Outer Carpathian orogenic belt thrusting over the North European Platform (Ślącza et al., 2006;
106 Oszczytko, 2006).



107
 108 **Fig. 2. A: Generalised geological map of the Polish part of the Carpathians based on Cieszkowski et al.,**
 109 **2017 and cited there, faults after Lexa et al., 2000. B: Main tectonic units under the Carpathians, after**
 110 **Żelaźniewicz et al., 2011.**

111
 112 **3.2 Analysis of the sectors**

113 We used the morphometry subdivision of Poland (Solon et al., 2018) to define the area, based on the
 114 subprovinces of the Western Outer Carpathians in the area of Poland and a small band of Northern Subcarpathia
 115 subprovince to the border of the Carpathians in the geological meaning (Carpathian overthrust on the Foredeep
 116 sediments), according to Lexa et al. (2000). The subdivision of the outer Carpathian belt is mostly used in the
 117 geology basis on the tectonostratigraphic units (nappes). This subdivision, however, does not allow differences
 118 in lineament systems parallel to the belt to be caught. The newly proposed morphostructural subdivision of the
 119 Western Carpathians (Minár et al., 2011) is another approach that compiles geological and morphological
 120 features. The Polish part of the Western Carpathians is subdivided into the following subregions (number
 121 according to the paper cited): (3f) Moravian–Silesian Beskid, (3a) Beskid Żywiecki–Gorce, (3b) Beskid
 122 Sądecki–Levočské vrchy, (5a) Beskid Wyspowy, (5b) Low Beskid and (6) North Foreland. The last subregion
 123 spans all the length of the northern Carpathian boundary between the Orava and San rivers. We decided to
 124 compile the geological subdivision with the morphological one (Solon et al., 2018), which also comprises a
 125 subdivision of the outermost units, into five sectors (Fig. 3, Tab. 1). The only change was including Mount
 126 Cicień in Beskid Wyspowy into the Central Silesian sectors, as this massif, unlike all other Beskid Wyspowy
 127 culminations is built of Silesian series deposits (Burtan, 1974).



128
 129 **Fig. 3. Sectors defined based on the physiogeographical (Solon et al., 2018) and tectonic subdivisions**
 130 **(Golonka et al., 2021) of the study area (Western Outer Carpathians in Poland).**

131
 132 **Tab. 1. Analyse sectors**

Analyszed sectors	Symbol	Mesoregions covered according to Solon et al., 2018
Western Silesian with Foremagura	WS	Silesian Beskid Mts., Żywiec Basin, Silesia Foothills, Mały Beskid Mts.
Central Silesian	CS	Wieliczka Foothills, Wiśnicz Foothills, Beskid Wyspowy Mts – only the Ciecień ridge, Rożnów Foothills, Ciężkowice Foothills, Gorlice Basin
Eastern Silesian and Skole	ES	Przemyśl Foothills, Jasło-Krosno Basin, Strzyżów Foothills, Dynów Foothills, Jasło Foothills, Bukowiec Foothills
Western Magura	WM	Orawa-Jordanów Foothills, Orawa Interfluve, Koniaków Intermontane Region, Żywiec-Kysuce Beski, Pewel-Krzeczów Ranges, Makowski Beskid, Żywiec-Orawa Beskid
Central Magura	CM	Sącz Beskid Mts., Sącz Basin, Wyspowy Beskid (without Ciecień Ridge), Gorce Mts.
Eastern Magura and Dukla	EM	Low Beskid Mts.

133
 134 **4. Digital elevation model**
 135 The Global Multi-resolution Terrain Elevation Data 2010 (GMTED2010; see Danielson, 2011) 7.5 arc-second
 136 product was chosen as a work base. The model is a compilation of different raster-based elevation sources, based
 137 mainly on SRTM digital terrain elevation data. The resolution is ca. 0.0021°/pixel, which means ca. 233 m/pixel.

138 This was found to be sufficient, while the working scale during lineament detection was 1:150 000. As the
139 shading azimuth can influence the results, the working imagery was multidirectional hillshade (Nagi, 2022).

140 **5. Methods**

141 **5.1 Multiple cover lineament detection**

142 The manual method of lineament extraction was applied for two reasons. First, it is the simplest, low cost and
143 widely used method. The second reason is that it creates a basis for further work, based on automated extraction.
144 However, the method used is prone to some operator-related bias (Scheiber et al., 2015; Ehlen, 2004). Thus, to
145 reduce this bias the lineaments were extracted by two operators working independently, in three sessions,
146 separated by intervals of several months. After each session, the results were analysed and a network of common
147 features was created. Lineaments marked by both operators were merged into single feature. Lineaments marked
148 by only one operator were removed. The last stage was creating a concise network of lineaments based on the
149 results of the three sessions.

150

151 **5.2 Network analysis**

152 A network can be described by scale-independent topological characteristics, based on the case of a line network
153 on graph theory. The network (graph) is formed by nodes (end or intersection points) connected by lines
154 (Sanderson and Nixon, 2015; Mukherjee, 2019). The line can be formed by one or more branches connected by
155 nodes. The node can be isolated (I type), an embranchment (Y type) or an intersection (X type), where the latter
156 two types are connecting nodes. Thus, the branch can connect two I type nodes (I–I branch), isolated and
157 connecting nodes (I–C branch, which can be I–Y or I–X) and two connecting nodes (C–C branch, which can be
158 X–X, X–Y or Y–Y). The proportion of nodes and branch types can be analysed as tertiary systems that
159 characterise the properties of the network, especially its interconnectivity (Procter and Sanderson, 2018;
160 Sanderson and Nixon, 2015; Sanderson et al., 2018).

161 The spatial variation of the topological parameters of the network was analysed with the following aspects: (1)
162 regular, in a 5x5 km grid; and (2) within sectors based on the mesoregions of physiogeographical subdivision,
163 according to Solon et al. (2018) and the main tectonic units (Fig. 3 Tab. 1).

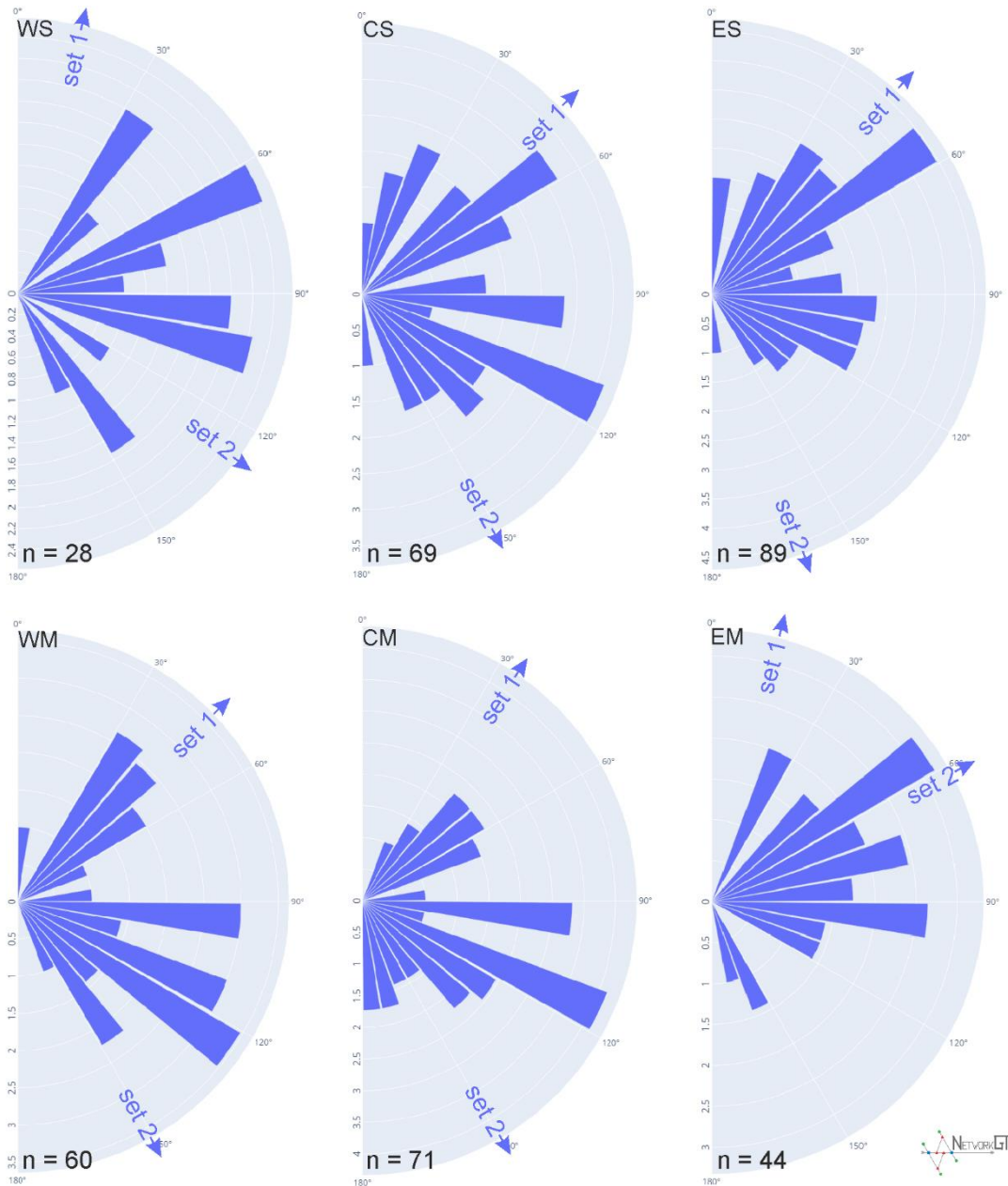
164 The NetworkGT Qgis toolbox (Nyberg et al., 2018) was used as a tool in the topological analyses. The lineament
165 network was checked and repaired with NetworkGT tools. An additional stage was the manual correction of
166 some features to eliminate all non-defined types of nodes, as well as some extremely short (ca. 500 m or shorter)
167 features. The topological parameters were analysed in three modes: the whole network; the sectors defined; and
168 in a regular, 5x5 km grid with 10 km search radius.

169 The Rayleigh test of semicircular distribution test was performed with the EZ-ROSE spreadsheet (Baas, 2000),
170 and circular statistics were calculated with the SciPy stats module (The SciPy Community, 2022).

171 **6. Results**

172 **6.1 Network geometry**

173 The azimuths of the lineaments in all the analysed sectors show a multimodal distribution. Thus, the directions
174 were separated into sets, in a way that gives low values of circular variance. The angular ranges of all the sets are
175 presented in Tab. 2. For all sets, except for set 2 in the Eastern Magura (EM) sector and set 2 in the Western
176 Silesian (WS) sector, the distribution is not uniform, as checked with the Rayleigh test (Baas, 2000). The two
177 sets not checked were not numerous enough to be representative.



178 **Fig. 4: Rose diagrams of the analysed networks in the analytic sectors; upper row: Western Silesian sector**
179 **with Foremagura (WS), Central Silesia (CS), Eastern Silesia with Skole (ES); lower row: Western Magura**
180 **(WM), Central Magura (CM), and Eastern Magura with Dukla (EM). Arrows mark the mean azimuth for**
181 **the sets defined in Tab. 2.**
182

183

184 **Tab. 2. Azimuths of the lineaments in the analyse sectors. All angles in degrees.**

Analyse sector	Set	Azimuths range	n	Circular statistics			The acute angle between sets means
				Mean	Std. dev	Variance	
CS	1	0 – 100	15	46.5	14.2	3.5	75.5
	2	100 – 180	13	151	16.6	4.8	
CM	1	0 – 80	17	34.1	13	3	63.9
	2	80 – 180	51	150.2	21.5	8.1	
EM	1	45 – 75	41	62.1	7.5	1.0	47.7
	2	0 – 45 75 – 180	3	14.4	26.7	12.5	
ES	1	0 – 100	59	42.7	19.7	6.8	62.1
	2	100 – 180	28	160.6	14.7	3.8	
WM	1	0 – 100	20	46.5	14.2	3.5	75.5
	2	100 – 180	40	151	16.6	4.8	
WS	1	0 – 60 150 – 180	23	13.6	23.3	9.5	66.2
	2	60 – 150	5	127.4	8.9	1.4	

185
 186 The orientation of lineaments in all sectors, as well as the circular mean azimuth are shown in Fig. 4. In sectors
 187 Central and Eastern Silesian (CS, ES) and Central and Western Magura (CM, WM) the set 1 mean is located
 188 between 34° and 47°, marking a dominant SW–NE strike of lineaments. In the Western Silesian sector (WS), set
 189 1 is oriented more to the north (14°). In all sectors above, there is a second set with a NW–SE trend, mostly
 190 oriented at 150–160°, but in the Western Silesian sector case the mean azimuth is lower (127°), as in the case of
 191 the first set. The last sector, Eastern Magura and Dukla, is different. There is one dominant set with azimuth 62°,
 192 and the second set is poorly represented and oriented northward. The angle between the two sets varies in the
 193 62–76° range, except in the Eastern Magura and Dukla sector where it is only 48°.

194 **6.2 Network topology**

195 In the study area, 305 lineaments were marked in total. These features comprise 432 nodes. Of this count, 58%
 196 are I nodes, 19% are E nodes, 18% are Y nodes and 5% are X nodes. The network contains 338 branches, within
 197 which 49% are C–I type branches, 29% are C–C branches and 22% are I–I branches marking completely
 198 separated lineaments. Topological parameters are shown in Tab. 3.

199

200 **Tab. 3. Topological parameters of the network in analyse sectors**

	Western Silesian with Foremagura	Central Silesian	Eastern Silesian and Skole	Western Magura	Central Magura	Eastern Magura and Dukla	Whole area

	WS	CS	ES	WM	CM	EM	
No. of nodes (I+X+Y)	19	68	101	47	67	40	383
I nodes	8	51	76	26	48	36	293
X nodes	1	6	6	3	6	2	19
Y nodes	10	11	21	18	15	2	71
E nodes	22	38	49	46	61	52	-
C-C connections	11.5	14.5	18.5	21.0	33.5	3.0	77.0
C-I connections	8.5	28.5	35.5	22.0	25.0	11.5	131.0
I-I connections	1.0	11.0	23.5	3.0	14.0	10.5	81.0
No. of branches	21.0	54.0	77.5	46.0	54.5	25.0	291
No. of lines	9.0	31.0	48.5	22.0	31.5	19.0	182
No. of connections	11	17	25	21	19	4	90
Connects per line	2.44	1.10	1.03	1.91	1.21	0.42	0.99
Connects per branch	1.62	1.06	1.02	1.43	1.12	0.56	0.99
Dim.less intensity	1.21	0.87	1.21	1.65	1.33	2.06	0.75
Av. Degree of network	2.21	1.59	1.53	1.96	1.63	1.25	1.52

201

202

203 The highest dimensionless intensity parameter is in the Eastern Magura and Dukla sector (2.05) and the lowest in
204 the Central Silesian (0.87). On the other hand, the Eastern Magura sector is characterised by the lowest
205 connections per branch (0.56) or the average degree of network (1.25) due to its form of mainly parallel features,
206 with only 12% of the branches of connecting type (C–C). The best interconnectivity is observed in the Western
207 Silesian sector with 1.62 connections per branch and an average degree of the network of 2.21. This is an effect
208 of the presence of the Żywiec Basin block-system in the central part of the region.

209 The difference between these two (Eastern Magura and Western Silesia) sectors can be clearly visible on the
210 ternary diagrams (Fig. 5) presenting the relationships of the nodes and branch types. In the Western Silesian
211 sector, there is a high ratio of Y type nodes (52% of non-E-type nodes) and only one I–I branch.

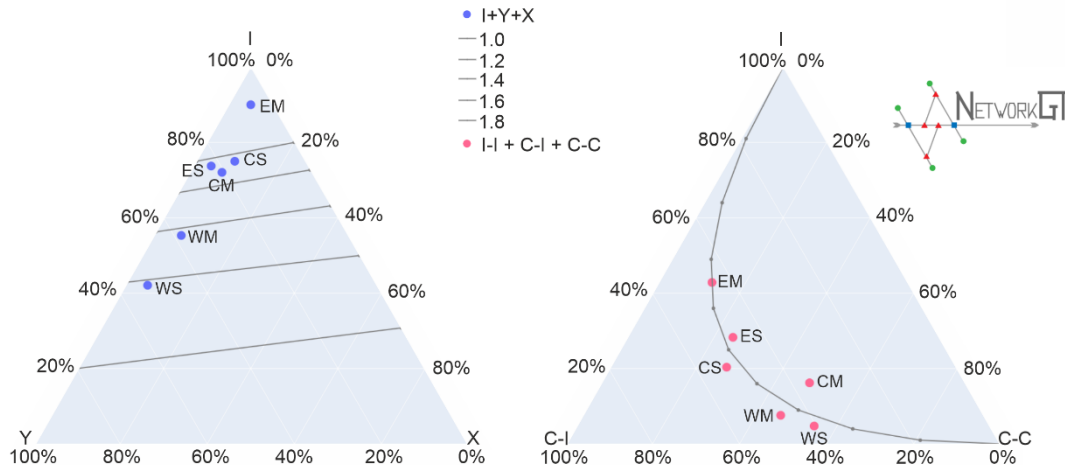


Fig. 5: Ternary diagram presenting nodes (left) and branches (right) proportions in the analyzed sectors.

The parameters of all the other sectors fall between the Eastern Magura and Western Silesian sectors. The Western Magura sector has quite good interconnectivity with a similar type of Eastern Magura blocky network. Another approach to analysing topology is to use a sampling regular grid. The results are shown in Fig. 5 as maps of connections per branch number, 2D network intensity and dimensionless intensity.

It can be seen we have two relatively large regions with a high value of connections per branch parameter. The first one is in the Western Silesian and partially Western Magura sectors, that is, the Żywiec Basin area, but from the geological point of view it is also a narrow zone of Foremagura units occurring between the Silesian and Magura nappes. Moreover, the Subsilesian unit tectonic window occurs in this area.

The Nowy Sącz Basin (eastern part of the Central Magura sector in the subdivision used here) is the next region with a high number of connections per network branch. The lineament system in this area surrounds a zone of Neogene deposits lying on the Carpathian flysch and filling the intramountain Nowy Sącz Basin.

The 2D intensity map shows that the Nowy Sącz Basin is characterised in general by a higher intensity than the Żywiec Basin. There is also a general trend of higher intensity in the western part of the Carpathians (especially the Western Magura and Central Magura sectors) than in the eastern part (Eastern Magura and Dukla).

In terms of dimensionless intensity parameter there are two regions with significantly high values: the south-eastern part of the Wiśnicz foothill, which is in the Central Silesian sector, and the eastern parts of the Beskid Niski Mts. and Bukowiec foothill in the Eastern Magura and Eastern Silesian sectors, on the geographical border of the Western and Eastern Carpathians.

7. Discussion

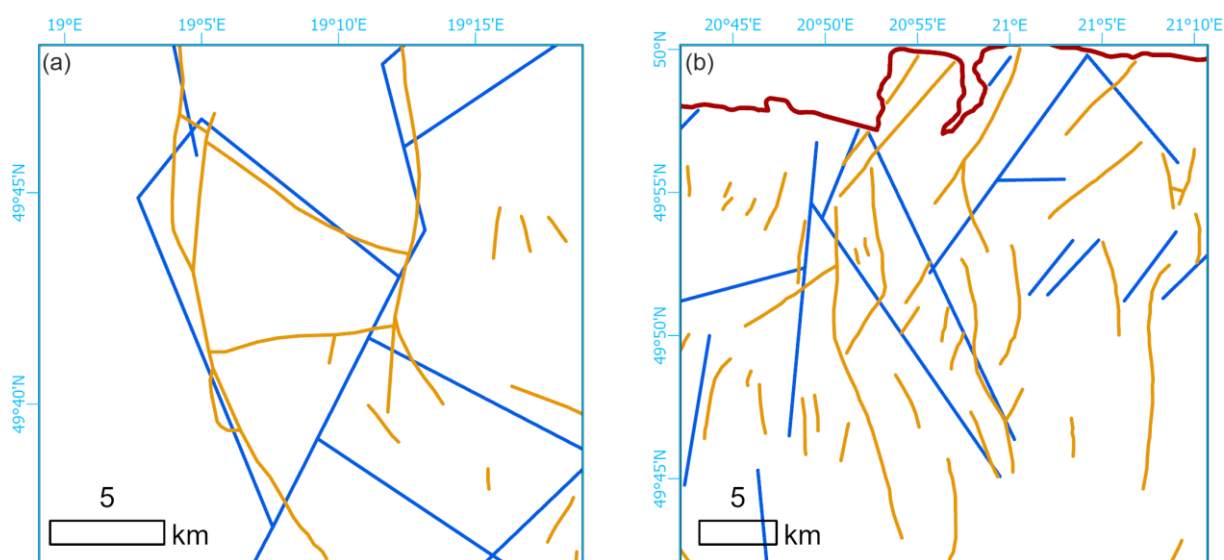
7.1 Different lineament identification approaches

There are 110 photolineaments marked on the photogeological map of Poland in the studied area (Bażyński et al., 1986). In the same area of the geological map of the Carpathians, Lexa et al. (2000) marked 2 325 features described as a fault or assumed fault. In many cases, our lineament system seems to be concordant or complimentary to Lexa et al.'s (Fig. 6). In some cases, the features marked as faults are rather thrust lines, as per the Fig. 6a example. The photolineament system is in general concordant with the DEM-interpreted system.

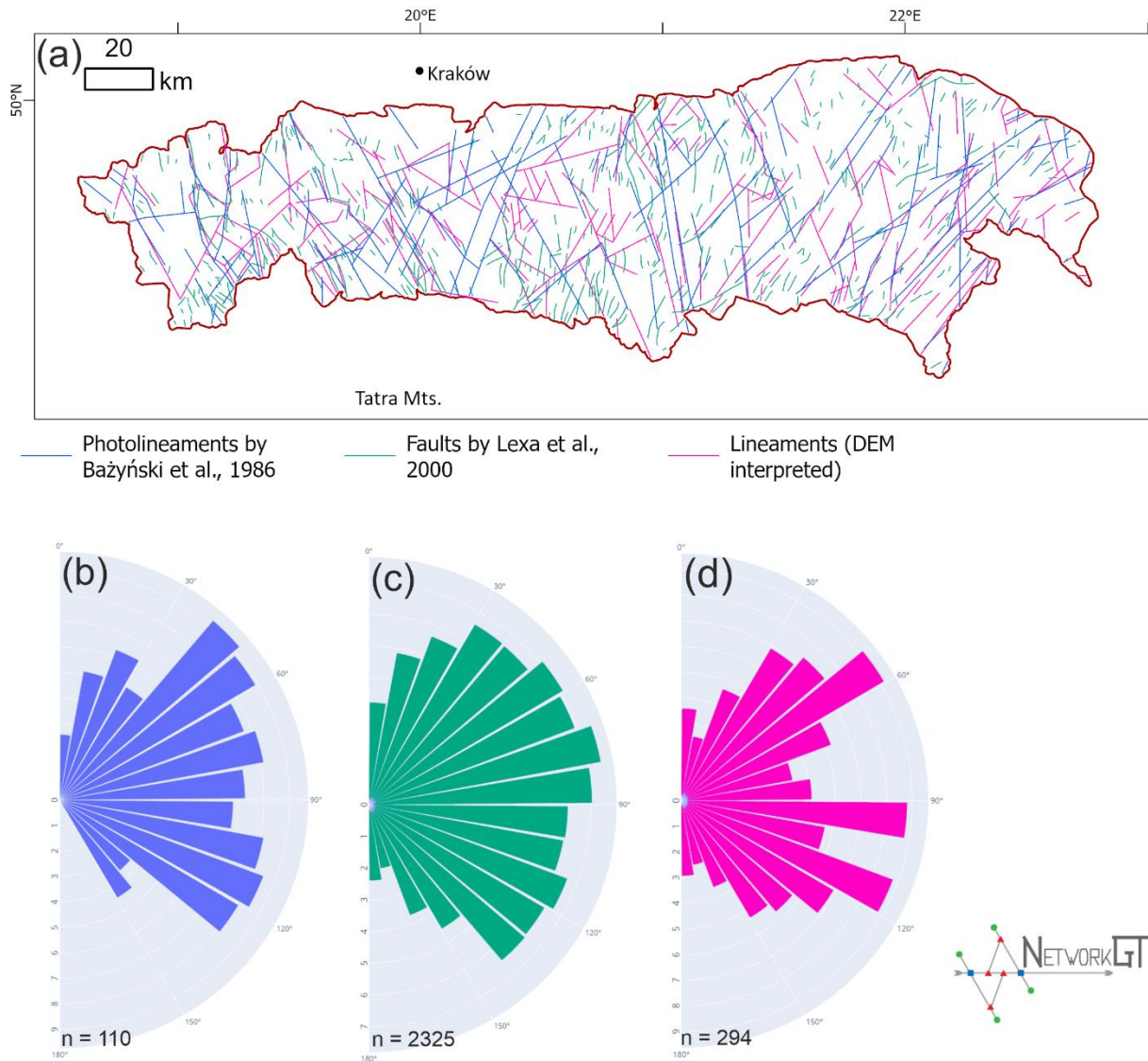
Visual inspection of the compiled lineaments map (Fig. 7a) shows that the especially NE striking lineaments of

241 the Eastern Magura sector are consistent with each other. Moreover, the system framing the Żywiec tectonic
 242 window is well visible in both sets. On the other hand, there are some photolineaments that are not recognisable
 243 on the DEM, and in fact also hardly visible on the modern orthophoto map. The most prominent example are two
 244 straight, parallel lineaments striking the NNE in the central part of the study area, cutting its entire width. These
 245 features seem to cut Gorce Mts.; this is not confirmed by our other studies (Kania and Szczęch, 2020; Szczęch
 246 and Cieszkowski, 2021). Further to the north, these two lineaments are delimiting massifs of the Beskid
 247 Wyspowy Mts. (Mogieliica, Łopień). These massifs are in fact particularly visible on the aerial photo, as rather
 248 isometric ‘islands’, and are formed by core parts of the synclines (Wójcik et al., 2009). On the other hand, some
 249 lineament systems well visible in DEM are not marked on the photolineament map, as per the case of the system
 250 north of the Nowy Sącz. That shows how these two methods can in fact be recognised as complementary
 251 approaches to the lineaments’ identification.

252 The system from the map by Lexa et al. (2000) shows confirmed and inferred faults, which is why it is not fully
 253 compatible with lineaments; the lineaments, even when mainly tectonic related, are in fact a broader term
 254 (O’Leary et al., 1976). Especially, these data, despite being a very rich collection of features are not applicable
 255 for topological analyses: most of the features are short and isolated even when forming a network. Nevertheless,
 256 these data include faults that are identified with geological criteria that are not visible in the remote sensing (at
 257 least at the scale applied in this paper or by Bażyński et al., 1986 photolineament map. These data are
 258 augmenting each other, which is highly visible in the Piwniczna Zdrój area, where DEM interpreted that the
 259 NNW striking lineament along the Poprad River Valley (not present in the photolineament set) is flanked with a
 260 set of N or NNE striking faults, which we have not identified on the DEM.



261
 262 **Fig. 6. Comparison of lineament system detected from the GMTED2010 model (blue) and faults by Lexa**
 263 **et al., 2000 (orange). (a) Żywiec Basin area, (b) fragment of the Zakliczyn – Olszyny fault zone.**



264
 265 **Fig. 7. Geometry of lineament networks in the Carpathians. (a) compilation map of lineaments by**
 266 **Bażyński et al., 1986, faults by Lexa et al., 2000 and lineaments interpreted from DEM in the presented**
 267 **paper. (b-d) roset diagrams of features azimuth in the whole study area from: (b) Bażyński et al. (1986), (c)**
 268 **Lexa et al., 2000 and (d) DEM interpreted.**

269
 270 When analysing the distribution of feature azimuth for the whole study area (Fig. 7b-d), it can be noted that the
 271 directions for the photolineament set (B) and DEM-interpreted set (D) are quite similar. What is noteworthy is
 272 the lack of azimuths greater than 150° in the photo set, which are present (albeit in a minority) in the DEM set.
 273 Furthermore, the photo set shows two maxima, at ca. 45° and 110°, whilst in the DEM set there are three
 274 maxima at ca. 50°, 100° and 110°. However, the dominating directions are not in fact distributed uniformly
 275 along the W–E span of the Polish Western Carpathians, which can be clearly seen in Fig. 7a where the
 276 domination of NE directions in the eastern sectors can be noticed, as well as the presence of two main directions
 277 in the western and central sectors.

278 **7.2 Dominating directions of the lineament network**

279 We observed a difference in dominating azimuths of lineaments between the western/central sectors (WS, WM,
280 CS, CM) and eastern sectors (ES, EM) of the study area. The first ones are characterised by two distinct sets of
281 lineaments (NNE or NE and SE), while the second has an SE set that is strongly reduced.

282 According to the general tectonic model of the Outer Carpathians (Unrug, 1980), the flysch deposits are cut by
283 set sinistral strike-slip fault zones. These fault zones are arranged in a fan-like shape along the arc of the
284 Carpathians, leading to the rotation of the set of nappes (Unrug, 1980; Graniczny and Mizerski, 2003). The
285 observed trend of increasing importance of the NE direction to the east is consistent with this model. However,
286 the more complicated geometry of the western part of the network may be related to the more complicated
287 system of the deep-rooted fault zones in this part (see further discussion below).

288 **7.3 Topological differentiation of the network**

289 There are no topological analyses of the lineament networks for the Outer Carpathians. Our previous article
290 (Kania and Szczęch, 2022) was focused on one mountain massif: Gorce Mts. From the tectonic point of view,
291 this massif is quite homogenous, being located in the one tectono-facial unit (Magura unit) with some subunits
292 within (Bystrica and Krynica subunits). Therefore, the paper focused mainly on different lithostratigraphic units,
293 showing how different types of lithology differ in topology terms.

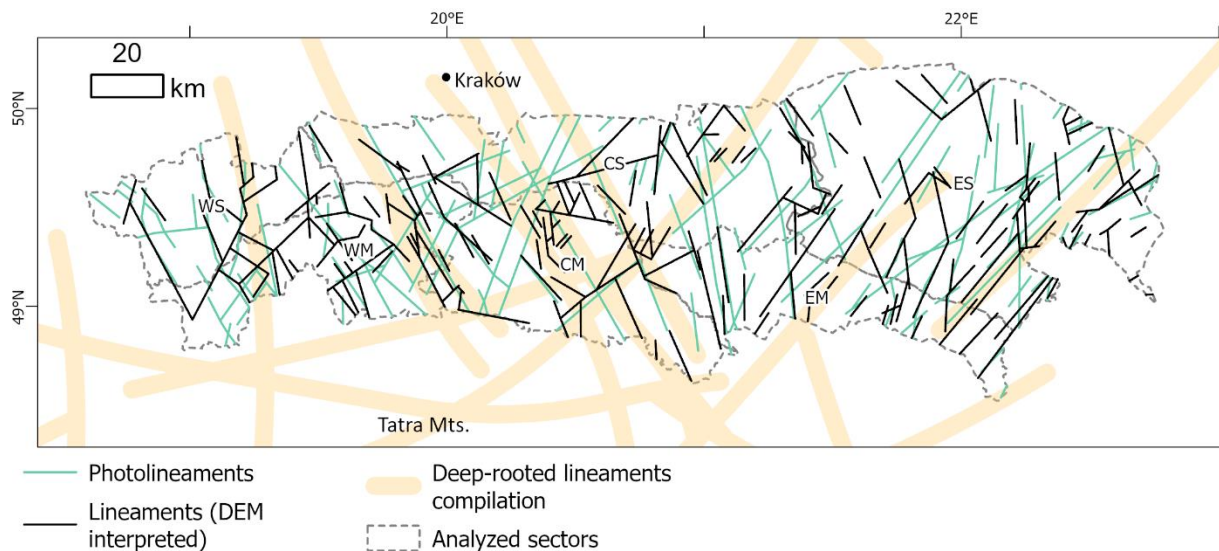
294 Scaling the research into the Polish Western Carpathians shows that in general there are no differences in the
295 network topology related to the tectono-facial units (Outer Carpathian nappes) since in general, all these units are
296 similar in lithology (flysch packets). However, there are differences related to some irregularities in tectonics:
297 especially, the intramountain basins are marked with increased network interconnectivity. The western part of
298 the study area in general has a better developed network. Especially, the Eastern Magura differs from the rest of
299 the sectors: the domination of one lineament direction results in low network interconnectivity, which is
300 expressed by a high proportion of the I nodes and I-I branches (Fig. 5). We analysed Magura unit and part of
301 the Dukla unit together; however, the interconnectivity in the Dukla Nappe (belonging to the Foremagura group)
302 is stronger than in Magura, which can be related to the proximity of the Silesian unit overthrust.

303 The highest interconnectivity was observed in the Western Silesian sector. The area is characterised by a high
304 proportion of Y nodes, and thus mainly by the presence of C-I or C-C branches (Fig. 5). In the geological
305 context, it is related to the location of the Żywiec tectonic window, which exposes the Subsilesian unit.

306 However, the topological study shows that the tectonised zone is wider; the increase in connections per branch
307 zone continues to the south along the Soła River and further, at least to the state border in the Beskid Żywiecki
308 Mts.

309 **7.4 Main large-scale, deep-rooted lineament systems of the Western Carpathians and their** 310 **relation to DEM-interpreted lineaments**

311 The following, well-known, large-scale lineaments reach the Carpathian basement cutting the Polish part of the
312 Outer Western Carpathians (Doktór et al., 1985): Central Slovakia, Myjava, Muran, Štitník and Przemyśl. There
313 are also lineaments not named by Doktór et al. (1985), but striking parallel, approximately 10 km to the east
314 from the Skawa fault zone (Cieszkowski et al., 2006). Fig. 8 presents the generalised positions of the lineaments.



315

316 **Fig. 8. Interpreted lineament system with photolineaments by Bażyński et al., 1986 as well as deep-rooted**
 317 **lineament compilation after Sikora, 1976; Zuchiewicz, 1984; Doktór et al., 1985. Important deep-rooted**
 318 **lineaments mark with numbers: 1 – Central Slovakia, 2 – Pericarpathian, 3 – Kraków – Prešov, 4 –**
 319 **Štitník, 5 – Myjava, 6 – Muran, 7 - Przemyśl**

320

321 The central Slovak line marks the eastern border of the Żywiec basin and marks the major fault zone well visible
 322 in the displacing Fore–Magura belt near Żywiec. Some of the lineaments belonging to the system can also be
 323 traced to the east, with some connecting NE–SW branches near the northern margin of the Carpathians.

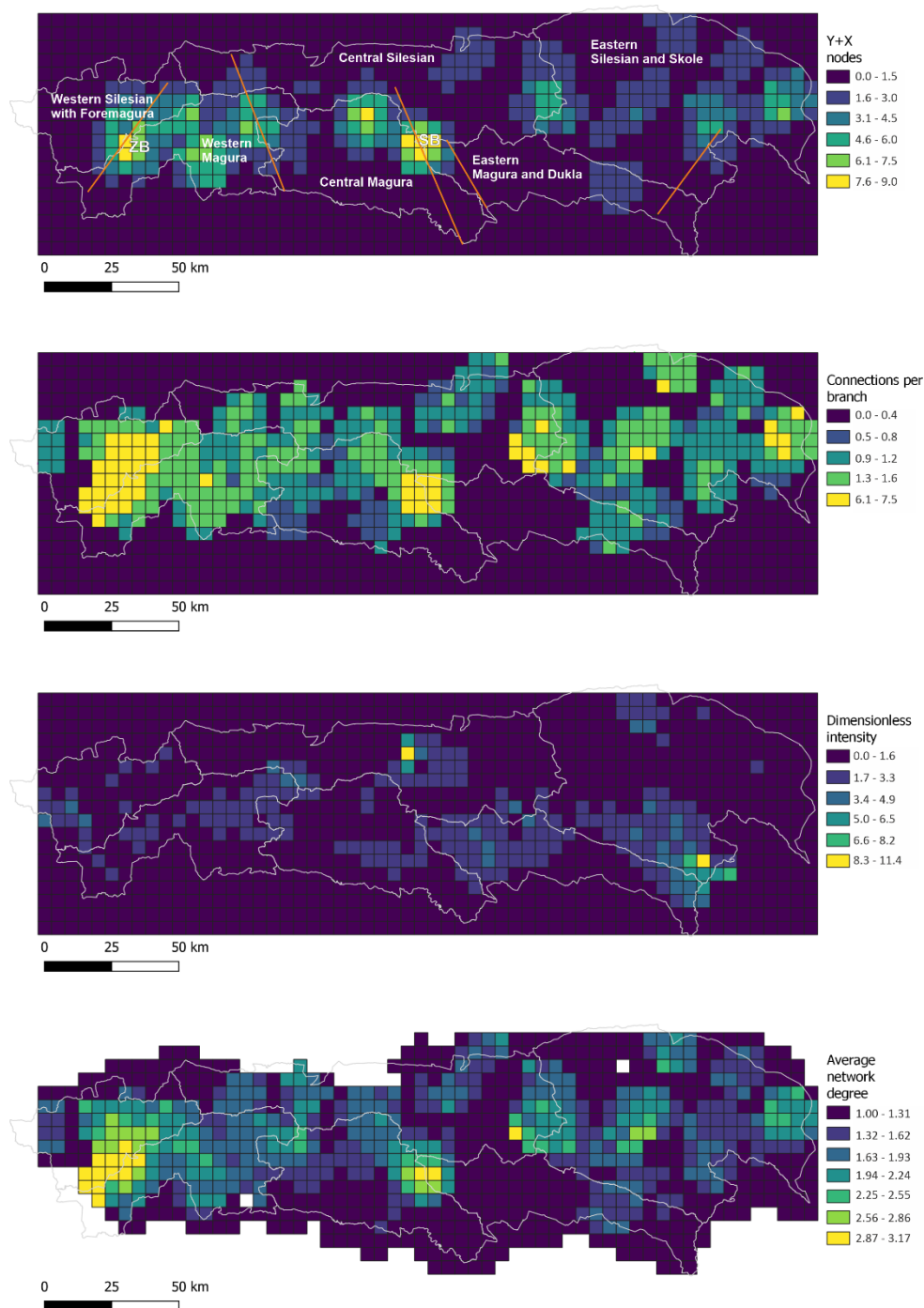
324 The system of Muran lineaments in the discussed region is marked by a few short NE–SW lineaments in the
 325 eastern sectors of the Magura and Silesian units. The Myjava system, in fact one of the most prominent systems
 326 in the Carpathians, in the study area can be traced along the Nowy Sącz Basin, continuing to the north where
 327 there is a series of short lines parallel to the zone lineaments. The network interconnectivity increases in this
 328 area. The lineaments there lie in an extension of the Carpathian Shear Corridor, a large-scale strike–slip zone
 329 between Vienna and the High Tatra Mts. (Marko et al., 2017). Although the Štitník system is unclear, some
 330 parallel or subparallel lineaments can be assigned to this zone. The Przemyśl lineament zone is identified as a set
 331 of long lineaments in the easternmost parts of the area, where the main features of NE–SW are possibly
 332 interconnected by shorter N–S lines, forming an interconnected, blocky, two-set system.

333 Another important deep-rooted linear structure, confirmed by a negative gravimetric anomaly is the
 334 Pericarpathian line, which runs along the Nowy Sącz–Nowy Targ–Kysucké Nové Mesto line (Zuchiewicz, 1984;
 335 Sikora, 1976), which runs similarly to the Myjava structure. The Kraków–Prešov lineament, which is an
 336 extension of the Kraków–Lubliniec fault zone and marks the border between the Małopolska and
 337 Brunovistulicum blocks of the basement (Žaba, 1999; Zuchiewicz, 1984). A system of lineaments is clearly
 338 visible along this line, mainly in the Magura Nappe; however, parallel photolineaments were marked even longer
 339 to the north (Bażyński et al., 1986).

340

341 These systems can be arranged in two sets: NNW, NW–SSE, SE striking (Central Slovakia, Skawa, Kraków–
 342 Presov and Štitník); and NE–SE (Myjava and Pericarpathian, Muran and Przemyśl). That implies some points of
 343 system intersection, and in the area analysed such a place is in the Nowy Sącz region. This place is characterised

344 by higher interconnection factors (Fig. 9), in relation to the surrounding area. Moreover, in terms of
 345 geomorphology, this is an intramountainous basin, being the only location where deposits are observed in the
 346 Magura Nappe Neogene.

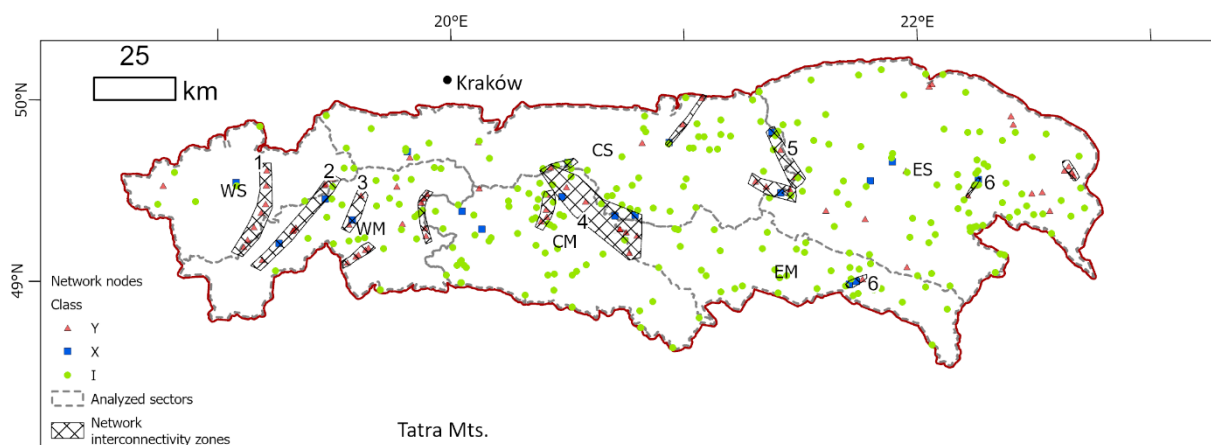


347
 348
 349 **Fig. 9. Topological parameters of the lineament network, from top to bottom: connecting nodes number,**
 350 **connections per branch number, dimensionless intensity factor, and average network degree. ZB – Żywiec**
 351 **Basin (Żywiec tectonic window), SB – Nowy Sącz Basin, lines on X-Y nodes map are main faults.**
 352

353 The Central Slovakian system strikes along the east border of the Żywiec Basin and Żywiec tectonic window,
 354 where the Subsilesian Nappe is exposed. We also marked a major lineament there, which is not present on the
 355 photolineament map (Bażyński et al., 1986) or the database of the Western Carpathian Geological Map (Lexa et
 356 al., 2000). The lineament (in the central part, the Soła River Valley) cuts the Magura Nappe, the Foremagura
 357 zone with Magura overthrust and the Silesian Nappe. This structure is one of the edges of the rhomboidal block,
 358 in which the Żywiec Basin has been developed. The generally increased degree of network interconnection (Fig.
 359 10) and the intensity of the network in this area can be an effect of the interaction between the central Slovakian
 360 system with the Soła lineament and all the lowered block edges.

361 The cross-cutting relations of the Myjava lineament and the Štitník lineament, whose continuation can be the
 362 Dunajec fault system, are reflected in the bimodality of lineaments. The dominating maximum in the central
 363 Magura sector, at approximately 120°, is similar to the Štitník lineament; however, the Myjava lineament is
 364 reflected there by just a few dominating lineaments, which are relatively long. Moreover, the Pericarpathian
 365 lineaments are also known in this region. This structure, reflected in the sedimentary cover as the Dunajec fault
 366 zone, is also confirmed by a negative gravimetric anomaly (Zuchiewicz, 1984; Sikora, 1976). Another deep
 367 structure cutting this area is the Kraków–Prešov fault, which is an extension of the Kraków–Lubliniec fault zone
 368 under the Carpathians active to the Quaternary (Żaba, 1999). All these deep cross-cutting features result in an
 369 increased degree of the network connectivity observed on the surface. Then, the blocky structure allowed the
 370 formation of an intramountain basin, filled with Neogene sediments.

371 Topological analysis also suggests that the well-known Skawa fault zone (Zuchiewicz et al., 2009; Unrug, 1980)
 372 is in fact the western-most part of the wider zone of increased network interconnectivity, extending ca. 10–20 km
 373 to the west of the Raba River. The final interpretation of correlation of lineaments increased interconnectivity
 374 areas with tectonic structures of the area is shown on the Fig. 10.



375
 376 **Fig. 10. Network nodes and zones of interconnectivity and their interpretation in context of Outer**
 377 **Carpathians Nappes (surface) and basement (deep) tectonics. 1 – Soła fault zone (surface), Central**
 378 **Slovakia lineament (deep), 2 – fault system along Sopotnia Valley, 3 – Skawa fault zone (surface), 4 –**
 379 **Nowy Sącz Basin (surface), Kraków – Prešov, Myjava and Štitník lineaments (deep), 5 – faults along**
 380 **Wisłoka Valley (surface), 6 – Muran lineament (deep).**

381
 382 The other aspect of the fault system of the Carpathians is occurrence and migration of the mineral waters. The
 383 area to the south of the Nowy Sącz there is a well-known region of CO₂-rich mineral waters occurrence with
 384 renowned spa sites. These waters are associated with fault zones, often the deep one, penetrating to the

385 crystalline basement of the Carpathians (Oszczypko and Zuber, 2002; Zuber and Chowaniec, 2009; Ciężkowski
386 et al., 2010). Its noteworthy, that this region is located on the crossing of two major deep-rooted fault zones:
387 Śitnik lineament and Myjava lineament (Fig. 8). Similarly, the deep faults can be patch of migration of
388 hydrocarbons, especially if source rocks are related to the platform cover of Brunovistulicum and Małopolska
389 Massif lying under the Carpathians. In fact, some of the Polish Carpathian gas deposits are related to the
390 Mesozoic-Palaeozoic basement (Kotarba and Koltun, 2006). Thus, the analyse of the fault systems and their
391 interconnectivity has the potential in study of both, hydrocarbon and hydrogeological systems.

392 **8. Conclusions**

393 The proposed data source and analysis method are complementary with other lineament analysis from the study
394 area. The observed azimuths are in general concordant with the photolineament network; however, there are
395 some structures that are not confirmed by DEM interpretation. The relationship between the DEM-interpreted
396 data and geologically confirmed faults shows the usefulness of DEM as a data source in fault detection.

397 The dominating directions of the network are typical for the Western Carpathians, with a clear increase of the
398 NE striking features proportion towards the east.

399 The topological properties of the lineament network in the Western Carpathians show E–W trends, but no clear
400 S–N (perpendicular to the tectonic units) trends. This justifies the proposed subdivision of the Carpathians in the
401 western, central and eastern sectors in addition to the tectono-facial subdivision. The eastern sectors are
402 dominated by NE–SW trends and low interconnectivity, while the central and western sectors are more
403 interconnected and characterised by cross-cutting relationships of two main lineament directions. The degree of
404 network interconnectivity increases in areas with a lower morphology (intramountainous basins): the Żywiec
405 Basin and Nowy Sącz Basin.

406 The geometry of the network, in general, reflects a system of deep-rooted lineaments. The cross-cutting area of
407 the main deep lineaments is reflected in stronger network interconnectivity in the Nowy Sącz area.

408
409 **CrediT authorship contribution statement:** Maciej Kania: Conceptualization, Methodology, Formal analysis,
410 Investigation, Writing – original draft, Visualization. Mateusz Szczęch: Investigation, Writing – review &
411 editing, Visualization.

412
413 **Declaration of competing interest:** The authors declare that they have no known competing financial interests or
414 personal relationships that could have appeared to influence the work reported in this paper

415
416 **Acknowledgements:** The research was financed from funds of the Jagiellonian University Institute of
417 Geological Sciences. The publication and proofreading of this publication has been supported by a grant from
418 the Priority Research Area (Digiworld) under the Strategic Programme Excellence Initiative at Jagiellonian
419 University. The authors would like to thank both referees, Prof. Fabrizio Balsamo and Prof. Jan Golonka for
420 their helpful comments improving a quality of the paper.

421 **References**

422 Baas, J. H.: EZ-ROSE: a computer program for equal-area circular histograms and statistical analysis of two-
423 dimensional vectorial data, *Computers & Geosciences*, 26, 153–166, [https://doi.org/10.1016/S0098-](https://doi.org/10.1016/S0098-3004(99)00072-2)
424 [3004\(99\)00072-2](https://doi.org/10.1016/S0098-3004(99)00072-2), 2000.

425 Barmuta, J., Starzec, K. and Schnabel, W.: Seismic-Scale Evidence of Thrust-Perpendicular Normal

426 Faulting in the Western Outer Carpathians, Poland, *Minerals*, 11:1252, <https://doi.org/10.3390/min11111252>,
427 2021. Bażyński, J., Doktor, S., and Graniczny, M.: Mapa fotogeologiczna Polski w skali 1:1 000 000, 1986.

428 Burtan, J.: Detailed Geological Map of Poland, 1:50 000 scale, Mszana Dolna sheet. Wydawnictwa Geologiczne,
429 Warszawa, 1974.

430 Chodyń, R.: Zastosowanie cyfrowego modelu terenu (DEM) w badaniach geologicznych na przykładzie obszaru
431 między Dobczycami a Mszaną Dolną (polskie Karpaty zewnętrzne), *Przegląd Geologiczny*, 52, 315–320, 2004.

432 Cieszkowski, M., Golonka, J., Waśkowska-Oliwa, A., and Chrustek, M.: Budowa geologiczna rejonu Sucha
433 Beskidzka – Świnna Poręba (polskie Karpaty fliszowe), *Geologia / Akademia Górniczo-Hutnicza im. Stanisława*
434 *Staszica w Krakowie*, 32, 155–201, 2006.

435 Cieszkowski, M., Kysiak, T., Szczęch, M., and Wolska, A.: Geology of the Magura Nappe in the Osielec area
436 with emphasis on an Eocene olistostrome with metabasite olistoliths (Outer Carpathians, Poland), *Annales*
437 *Societatis Geologorum Poloniae*, 87, 169–182, <https://doi.org/10.14241/asgp.2017.009>, 2017.

438 Ciężkowski, W., Chowaniec, J., Górecki, W., Krawiec, A., Rajchel, L. and Zuber, A.: Mineral and thermal
439 waters of Poland, *Przegląd Geologiczny*, 58, 762–773, 2010.

440 Danielson, J. J.: Global Multi-resolution Terrain Elevation Data 2010 (GMTED2010) Coastal Elevation
441 Modeling View project LP DAAC View project, 2011.

442 Doktor, S. and Graniczny, M.: Geologiczna interpretacja zdjęć satelitarnych i radarowych wschodniej części
443 Karpat, *Kwartalnik Geologiczny*, 26, 231–245, 1982.

444 Doktor, S. and Graniczny, M.: Fotogeologiczna analiza zdjęć satelitarnych Karpat, *Kwartalnik Geologiczny*, 27,
445 645–656, 1983.

446 Doktor, S., Dornic, J., Graniczny, M., and Reichwalder, P.: Structural elements of Western Carpathians and their
447 Foredeep on the basis of satellite interpretation, *Geological Quarterly*, 29, 129–138, 1985.

448 Doktor, S., Graniczny, M., Kucharski, R., Molek, M., and Dąbrowska, B.: Wgłębna budowa geologiczna Karpat
449 w świetle kompleksowej analizy teledetekcyjno-geofizycznej, *Przegląd Geologiczny*, 38, 469–475, 1990.

450 Doktor, S., Graniczny, M., Kowalski, Z., and Wójcik, A.: Możliwości zastosowania wyników interpretacji zdjęć
451 radarowych do analizy tektonicznej Karpat, *Przegląd Geologiczny*, 50, 852–860, 2002.

452 Ehlen, J.: Lineation, edited by: Goudie, A. S., *Encyclopedia of Geomorphology*, 2, 623–624, 2004.

453 Golonka, J., Aleksandrowski Paweł and Aubrecht, R., Chowaniec, J., Chrustek, M., Cieszkowski, M., Florek, R.,
454 Gawęda, A., Jarosiński, M., Kępińska, B., and others: The Orava deep drilling project and post-palaeogene
455 tectonics of the northern Carpathians, *Annales Societatis Geologorum Poloniae*, 75, 211–248, 2005.

456 Golonka, J., Waśkowska, A., and Ślącza, A.: The Western Outer Carpathians: Origin and evolution, *Zeitschrift*
457 *der Deutschen Gesellschaft für Geowissenschaften*, 229–254, 2019.

458 Golonka, J., Gawęda, A., and Waśkowska, A.: Carpathians, Reference Module in Earth Systems and
459 Environmental Sciences, in: Alderton, D. and Elias, S. A. (eds.): *Encyclopedia of Geology (Second Edition)*,
460 Academic Press, 372–381, <https://doi.org/10.1016/b978-0-12-409548-9.12384-x>, 2021.

461 Graniczny, M. and Mizerski, W.: Lineamenty na zdjęciach satelitarnych Polski – próba podsumowania, *Przegląd*
462 *Geologiczny*, 51, 474–482, 2003.

463 Kania, M. and Szczęch, M.: Geometry and topology of tectonolineaments in the Gorce Mts. (Outer Carpathians)
464 in Poland, *J Struct Geol*, 141, 104186, <https://doi.org/10.1016/j.jsg.2020.104186>, 2020.

465 Kania, M. and Szczęch, M.: Tectonic Structures Interpretation Using Airborne-Based LiDAR DEM on the
466 Examples from the Polish Outer Carpathians, in: *Atlas of Structural Geological and Geomorphological*
467 *Interpretation of Remote Sensing Images*, edited by: Misra, A. A. and Mukherjee, S., 157–165, 2022.

468 Kotarba, M.J. and Koltun, Y.V.: The Origin and habitat of hydrocarbons of the Polish and Ukrainian parts of the
469 Carpathian Province, in: Golonka, J. and Picha, F., *The Carpathians and Their Foreland: Geology and*
470 *Hydrocarbon Resources: AAPG Memoir*, 84, 321–368, 2006.

471 Książkiewicz, M.: The Tectonics of the Carpathians, in: *Geology of Poland*, vol. 4. Tectonics. The Alpine
472 Tectonic Epoch, Geological Institute, Warszawa, 476–608, 1977.

473 Leech, D. P., Treloar, P. J., Lucas, N. S., and Grocott, J.: Landsat TM analysis of fracture patterns: A case study
474 from the Coastal Cordillera of northern Chile, *Int J Remote Sens*, 24, 3709–3726,
475 <https://doi.org/10.1080/0143116031000102520>, 2003.

476 Lexa, J., Bezák, V., Elečko, M., Mello, J., Polák, M., and Vozár, J.: Geological map of western Carpathians and
477 adjacent areas 1:500 000, 2000.

478 Mahel', M.: Tectonics of the Carpathian–Balkan Regions, Explanations to the Tectonic Map of the Carpathian-
479 Balkan Regions and Their Foreland., Štátny geologický ústav Dionýza Štúra, Bratislava, 180–197 pp., 1974.

480 Marko, F., Andriessen, P. A. M., Tomek, Č., Bezák, V., Fojtíková, L., Božanský, M., Piovarči, M., and
481 Reichwalder, P.: Carpathian Shear Corridor – A strike-slip boundary of an extruded crustal segment,
482 *Tectonophysics*, 703–704, 119–134, <https://doi.org/10.1016/j.tecto.2017.02.010>, 2017.

483 Van der Meer, F. D., van der Werff, H. M. A., van Ruitenbeek, F. J. A., Hecker, C. A., Bakker, W. H., Noomen,
484 M. F., van der Meijde, M., Carranza, E. J. M., de Smeth, J. B., and Woldai, T.: Multi- and hyperspectral geologic
485 remote sensing: A review, <https://doi.org/10.1016/j.jag.2011.08.002>, 2012.

486 Minár, J., Bielik, M., Kováč, M., Plašienka, D., Barka, I., Stankoviansky, M., and Zeyen, H.: New
487 morphostructural subdivision of the Western Carpathians: An approach integrating geodynamics into targeted
488 morphometric analysis, *Tectonophysics*, 502, 158–174, 2011.

489 Motyl-Rakowska, J. and Ślącza, A.: Ważniejsze lineamenty Karpat i ich związek ze znanymi uskokami,
490 *Przegląd Geologiczny*, 32, 72–77, 1984.

491 Mukherjee, S.: Using Graph Theory to Represent Brittle Plane Networks, 259–271,
492 <https://doi.org/10.1016/B978-0-12-814048-2.00022-3>, 2019.

493 Nagi, R.: Introducing Esri's Next Generation Hillshade: [https://www.esri.com/arcgis-blog/products/arcgis-](https://www.esri.com/arcgis-blog/products/arcgis-living-atlas/imagery/introducing-esri-next-generation-hillshade/?rmedium=redirect&rsourc=blogs.esri.com/esri/arcgis/2014/07/14/introducing-esri-next-generation-hillshade)
494 [living-atlas/imagery/introducing-esri-](https://www.esri.com/arcgis-blog/products/arcgis-living-atlas/imagery/introducing-esri-next-generation-hillshade/?rmedium=redirect&rsourc=blogs.esri.com/esri/arcgis/2014/07/14/introducing-esri-next-generation-hillshade)
495 [hillshade/?rmedium=redirect&rsourc=blogs.esri.com/esri/arcgis/2014/07/14/introducing-esri-next-generation-](https://www.esri.com/arcgis-blog/products/arcgis-living-atlas/imagery/introducing-esri-next-generation-hillshade/?rmedium=redirect&rsourc=blogs.esri.com/esri/arcgis/2014/07/14/introducing-esri-next-generation-hillshade)
496 [hillshade](https://www.esri.com/arcgis-blog/products/arcgis-living-atlas/imagery/introducing-esri-next-generation-hillshade/?rmedium=redirect&rsourc=blogs.esri.com/esri/arcgis/2014/07/14/introducing-esri-next-generation-hillshade), last access: 1 June 2022.

497 Nyberg, B., Nixon, C. W., and Sanderson, D. J.: NetworkGT: A GIS tool for geometric and topological analysis
498 of two-dimensional fracture networks, *Geosphere*, 14, 1618–1634, <https://doi.org/10.1130/GES01595.1>, 2018.

499 O’Leary, D. W., Friedman, J. D., and Pohn, H. A.: Lineament, linear, lineation: Some proposed new standards
500 for old terms, *Geological Society of America Bulletin*, 87, 1463–1469, 1976.

501 Oszczytko, N.: Late Jurassic-Miocene evolution of the Outer Carpathian fold-and-thrust belt and its foredeep
502 basin (Western Carpathians, Poland), *Geological Quarterly*, 50, 169–194, 2006.

503 Oszczytko, N. and Zuber, A.: Geological and isotopic evidence of diagenetic waters in the Polish Flysch
504 Carpathians. *Geologica Carpathica*, 53, 257–268, 2002.

505 Ozimkowski, W.: Lineamenty otoczenia Tatr - porównanie interpretacji DEM i MSS, *Przegląd Geologiczny*, 56,
506 1099–1102, 2008.

507 Plašienka, D.: Continuity and episodicity in the early Alpine tectonic evolution of the Western Carpathians: How
508 large-scale processes are expressed by the orogenic architecture and rock record data, *Tectonics*, 37, 2029–2079,
509 2018.

510 Procter, A. and Sanderson, D. J.: Spatial and layer-controlled variability in fracture networks, *J Struct Geol*, 108,
511 52–65, <https://doi.org/10.1016/j.jsg.2017.07.008>, 2018.

512 Sanderson, D. J. and Nixon, C. W.: The use of topology in fracture network characterization, *J Struct Geol*, 72,
513 55–66, <https://doi.org/10.1016/j.jsg.2015.01.005>, 2015.

514 Sanderson, D. J., Peacock, D. C. P., Nixon, C. W., and Rotevatn, A.: Graph theory and the analysis of fracture
515 networks, *J Struct Geol*, 14th April, <https://doi.org/10.1016/j.jsg.2018.04.011>, 2018.

516 Scheiber, T., Fredin, O., Viola, G., Jarna, A., Gasser, D., and Łapińska-Viola, R.: Manual extraction of bedrock
517 lineaments from high-resolution LiDAR data: methodological bias and human perception, 137, 362–372,
518 <https://doi.org/10.1080/11035897.2015.1085434>, 2015.

519 Sikora, W.: On lineaments found in the Carpathians, *Rocznik Polskiego Towarzystwa Geologicznego*, 46, 3–37,
520 1976.

521 Sikora, R.: Geological and geomorphological conditions of landslide development in the Wisła source area of the
522 Silesian Beskid mountains (Outer Carpathians, southern Poland), *Geological Quarterly*, 66: 19,
523 <http://dx.doi.org/10.7306/gq.1651>, 2022.

524 Ślęczka, A., Kruglov, S., Golonka, J., Oszczytko, N., and Popadyuk, I.: Geology and hydrocarbon resources of
525 the Outer Carpathians, Poland, Slovakia, and Ukraine: general geology, in: Golonka, J. and Picha, F., *The*
526 *Carpathians and Their Foreland: Geology and Hydrocarbon Resources: AAPG Memoir*, 84, 221–258, 2006.

527 Solon, J., Borzyszkowski, J., Małgorzata Bidłasik, Richling, A., Badora, K., Balon, J., Brzezińska-Wójcik, T.,
528 Chabudziński, Ł., Dobrowolski, R., Grzegorzczak, I., Jodłowski, M., Kistowski, M., Kot, R., Krąż, P., Lechnio,
529 J., Macias, A., Majchrowska, A., Malinowska, E., Migoń, P., Myga-Piątek, U., Nita, J., Papińska, E., Rodzik, J.,
530 Strzyż, M., Terpiłowski, S., Ziaja, W., and Paul, J.: Physico-geographical mesoregions of Poland: verification
531 and adjustment of boundaries on the basis of contemporary spatial data, *Geographia Polonica*, 91, 143–170,
532 <https://doi.org/10.7163/GPol.0115>, 2018.

533 Szczęch, M. and Cieszkowski, M.: Geology of the Magura Nappe, south-western Gorce Mountains (Outer
534 Carpathians, Poland), *Journal of Maps*, 17, 453–464, <https://doi.org/10.1080/17445647.2021.1950579>, 2021.

535 Teisseyre, W.: O związku w budowie tektonicznej Karpat i ich przedmurza, *Kosmos*, 32, 393–402, 1907.

536 Statistics (scipy.stats) — SciPy v1.9.3 Manual: <https://docs.scipy.org/doc/scipy/tutorial/stats.html>, last access: 8
537 November 2022.

538 Thiele, S. T., Jessell, M. W., Lindsay, M., Ogarko, V., Wellmann, J. F., and Pakyuz-Charrier, E.: The topology
539 of geology 1: Topological analysis, *Journal of Structural Geology*, 91, 27–38,
540 <https://doi.org/10.1016/J.JSG.2016.08.009>, 2016.

541 Unrug, R.: Tectonic rotation of flysch nappes in the Polish Outer Carpathians, *Rocznik Polskiego Towarzystwa
542 Geologicznego*, 50, 27–39, 1980.

543 Valentini, L., Perugini, D., and Poli, G.: The “small-world” topology of rock fracture networks, *Physica A:
544 Statistical Mechanics and its Applications*, 377, 323–328, <https://doi.org/10.1016/j.physa.2006.11.025>, 2007.

545 Wójcik, A., Czerwiec, J., and Krawczyk, M.: Szczegółowa Mapa Geologiczna Polski 1:50 000. arkusz
546 Limanowa, 2009.

547 Yang, L., Meng, X., and Zhang, X.: SRTM DEM and its application advances,
548 <https://doi.org/10.1080/01431161003786016>, 2011.

549 Zuber, A. and Chowaniec, J.: Diagenetic and other highly mineralized waters in the Polish Carpathians, *Applied
550 Geochemistry*, 24, 1889–1900, 2009.

551 Zuchiewicz, W.: The late Neogene - Quaternary tectonic mobility of the Polish West Carpathians - a case study
552 of the Dunajec drainage basin, *Annales Societatis Geologorum Poloniae*, 54, 133–189, 1984.

553 Zuchiewicz, W., Tokarski, A. K., Świerczewska, A., and Cuong, N. Q.: Neotectonic Activity of the Skawa River
554 Fault Zone (Outer Carpathians, Poland), *Annales Societatis Geologorum Poloniae*, 79, 67–93, 2009.

555 Żaba, J.: Ewolucja strukturalna utworów dolnopaleozoicznych w strefie granicznej bloków górnośląskiego i
556 małopolskiego, *Prace Państwowego Instytutu Geologicznego*, 166, 1–162, 1999.

557 Żelaźniewicz, A., Aleksandrowski, P., Buła, Z., Kornkowski, P. H., Konon, A., Oszczypko, N., Ślęczka, A.,
558 Żaba, J. and Żytka, K.: Regionalizacja Tektoniczna Polski. Komitet Nauk Geologicznych PAN, Wrocław, 1–60
559 pp., 2011.

560

561